Eur. Phys. J. A (2021) 57:60
https://doi.org/10.1140/epja/s10050-021-00378-y

THE EUROPEAN PHYSICAL JOURNAL A

Regular Article - Theoretical Physics

Thermal study of a coupled-channel system: a brief review

Pok Man Lo[a]

Institute of Theoretical Physics, University of Wroclaw, 50204 Wrocław, Poland

Received: 31 May 2020 / Accepted: 3 February 2021 / Published online: 15 February 2021

Communicated by Laura Tolos

Abstract We demonstrate the construction of a density of states from the S-matrix describing a coupled-channel (S-wave $\pi\pi, K\bar{K}$) system, and examine the influences from various structures of particle dynamics: poles, roots, and Riemann sheets.

1 Density of states of a coupled-channel system

1.1 S-matrix formulation of statistical mechanics

The S-matrix theory provides a natural language to describe resonances and multi-channel dynamics. For the simple case of a single-channel, 2-body interactions, the scattering phase shift $\delta(E)$ uniquely identifies the density of states due to the presence of interactions, via an effective spectral function

$$B(E) = 2\frac{d}{dE}\,\delta(E). \tag{1}$$

This effective spectral function defines the thermodynamics of an interacting system [1–4]. For example, the thermal pressure due to the interaction can be computed as

$$\Delta P = \int \frac{dE}{2\pi}\, B(E)\, P^{(0)}(E,T) \tag{2}$$

where $P^{(0)}(E = m_a, T)$ denotes the pressure of an ideal gas of particles with mass m_a.

As energy increases, new interaction channel opens up and the scattering becomes inelastic. The S-matrix should be formally understood as a matrix acting in the space of open channels. The effective spectral function $B(E)$, in the case of a coupled-channel system, generalizes to [3]

$$\begin{aligned} B(E) &= \frac{1}{2}\mathrm{Im\,Tr}\left[S^{-1}\frac{d}{dE}S - \left(\frac{d}{dE}S^{-1}\right)S\right] \\ &= \frac{d}{dE}\,\mathrm{Im\ ln\,det}\,S(E). \end{aligned} \tag{3}$$

where S is an $N_{ch} \times N_{ch}$ scattering matrix of the coupled-channel system.

The quantity $B(E)$ summarizes the interactions among the scattering channels. Note that the trace operation (Tr) comes from the thermal trace in constructing the partition function. For example, while each S-matrix element represents a specific physical process, inelastic processes, expressed by off-diagonal terms, are included but only via the determinant. This poses strong theoretical constraints in model studies: when an inelastic process $\alpha \to \beta$ is considered, it is necessary to consider also the processes: $\beta \to \alpha$ and $\beta \to \beta$, on top of the elastic channel $\alpha \to \alpha$. Nevertheless, the trace operation implies that this quantity is basis independent, i.e., two S-matrices related by unitary rotations will give the same density of state. This also suggests that $B(E)$ does not depend explicitly on the inelasticity parameters.

Based on $B(E)$, an effective phase shift $\mathcal{Q}$ can be constructed:

$$\begin{aligned} \mathcal{Q}(E) &= \frac{1}{2}\int_{E_{\mathrm{ref}}}^{E} dE'\, B(E') \\ &= \frac{1}{2}\,\mathrm{Im\ ln\,det}\,\left(S(E)/S(E_{\mathrm{ref}})\right). \end{aligned} \tag{4}$$

$\mathcal{Q}$ generalizes the notion of a 2-body phase shift in Eq. (1) for describing dynamical processes. For example, it is defined even for a $3 \to 3$ scattering [3]:

$$\begin{aligned} \mathcal{Q}_3(E) &= \frac{1}{2}\,\mathrm{Im\ ln\,det}\left(I - 2\pi i \times \delta(E - \hat{H}_0)\,\hat{T}_3(E)\right) \\ &\approx -\frac{1}{2}\int d\phi_3\,\hat{T}_3(E) \end{aligned} \tag{5}$$

[a] e-mail: pmlo@gsi.de (corresponding author)

where $\int d\phi_3 \ldots$ is an integral over the 3-body phase space (on-shell). Note that some of the 3-body processes are built from iterating the 2-body ones (hence involving 2-body phase shifts), taking into account of such $\mathcal{Q}_3(E)$'s thus correspond to constructing the third coefficient in the cluster expansion based on those from the second ones. In addition, being a sum over the eigenphases of S, the effective phase shift $\mathcal{Q}(E)$ correctly includes the contributions from processes described by entries of the S-matrix. Conceptually it is an essential simplification: a single effective phase shift function can be constructed to describe the whole multi-channel system.

Determining the full N-body, multi-channel scattering matrix of an interacting system is in general very difficult (if not impossible). Rigorous theoretical schemes, such as chiral perturbation theory [5,6] and various functional methods, are effective in describing the low-energy limit and respecting symmetry constraints from chiral dynamics. Effective models [7] are adequate for channels dominated by a single, nearby resonance. Beyond these cases, inferring the density of states $B(E)$ from individual channels can be rather inefficient.

1.2 HRG approximation

A simple scheme for incorporating resonances in $B(E)$ is the hadron resonance gas (HRG) model [8,9]. Translating into the language of S-matrix, it corresponds to the approximation scheme

$$\mathrm{detS}(E) = \prod_{\{\mathrm{res}\}} \frac{z^{\star}_{\mathrm{res}} - E}{z_{\mathrm{res}} - E}, \tag{6}$$

where {res} is a table of resonances (e.g. from PDG) approximated as simple poles

$$z_{\mathrm{res}} \approx m_{\mathrm{res}} - i\,0^{+}. \tag{7}$$

$\mathcal{Q}_{\mathrm{HRG}}$ is then given by a sum over step-functions:

$$\mathcal{Q}(E) \to \mathcal{Q}_{\mathrm{HRG}}(E) = \sum_{\mathrm{res}} d_{IJ} \times (\pi \times \theta(E - \mathrm{m}_{\mathrm{res}})). \tag{8}$$

Note that resonances are incorporated in detS as product, reflecting the assumption that they are treated as independent.

The HRG approximation (8) is not a standard density expansion scheme. For example, while the $\rho-$ and $\omega-$ mesons are treated equally in the scheme, the former is identified as a 2-pion to 2-pion amplitude [4] (hence a term in second order virial expansion); while the latter is a 3-pion to 3-pion amplitude (or a quasi-elastic $\rho\pi \to \rho\pi$ process), belonging to the third order virial expansion in number of pions [10].

One key aspect to improving the approach is by including the widths of the resonances. Indeed, considerable theoretical efforts are involved in locating and characterizing resonance poles. Poles may be identified by analyzing the magnitude of $\det S(E)$. Nevertheless, Eq. (4) urges us to look at the phase of the $\det S(E)$. In the following, we shall study the phase function of the familiar 2-channel coupled-channel system of $(\pi\pi, K\bar{K})$. By directly graphing this function in the complex plane, we can read off the effective phase shift $\mathcal{Q}(E)$, and gain a robust comprehension of how the various S-matrix features: nearby poles, roots, cuts and effects of Riemann surfaces could influence the density of states.

2 DoS in a $\pi\pi$, $K\bar{K}$ coupled-channel system

We consider the coupled-channel model in Refs. [11–13] describing the interactions between the open channels $\pi\pi$ and $K\bar{K}$ (channel: $\alpha = 1, 2$), and in addition one closed-channel resonance state (channel: $\alpha = 3$), in the subspace of a fixed quantum number: $I = 0$, S-wave. Note that states with the same quantum number, respected by the Hamiltonian, will participate naturally in the coupled-channel system. A πK state, with quantum numbers $I = \frac{1}{2}, \frac{3}{2}$ and $|S| = 1$, will not enter this system directly, but a $(\pi\pi K\bar{K})$ would. (The thermodynamics of the former is treated in Ref. [14].) For thermal model applications, high-energy states are suppressed by the Boltzmann integral and hence we focus first on the two-channel case, each involves binary collisions. The calculation follows closely that in Ref. [11]. Some key steps will be repeated here. Refer to Ref. [15] for details.

2.1 Constructing the S-matrix

Our starting point is the free Green's function, which takes the form:

$$G^0(s) = \mathrm{diag}\left[G^0_{\pi\pi},\, G^0_{K\bar{K}},\, \frac{1}{s - M_R^2 + i\,0^{+}}\right] \tag{9}$$

where

$$\begin{aligned} G^0_{\alpha=1,2} &= 4\pi \int \frac{d^3k_1}{(2\pi)^3} \frac{1}{q_\alpha^2 - k_1^2 + i\,0^{+}}, \\ q_1^2 &= s/4 - m_\pi^2 \\ q_2^2 &= s/4 - m_K^2. \end{aligned} \tag{10}$$

The integral G^0_α is regulated by a form factor $\frac{1}{k_1^2+\mu_\alpha^2}$ The interaction term V describes the interactions among the open channels ($\alpha = 1, 2$) and their coupling to the resonance R($\alpha = 3$):

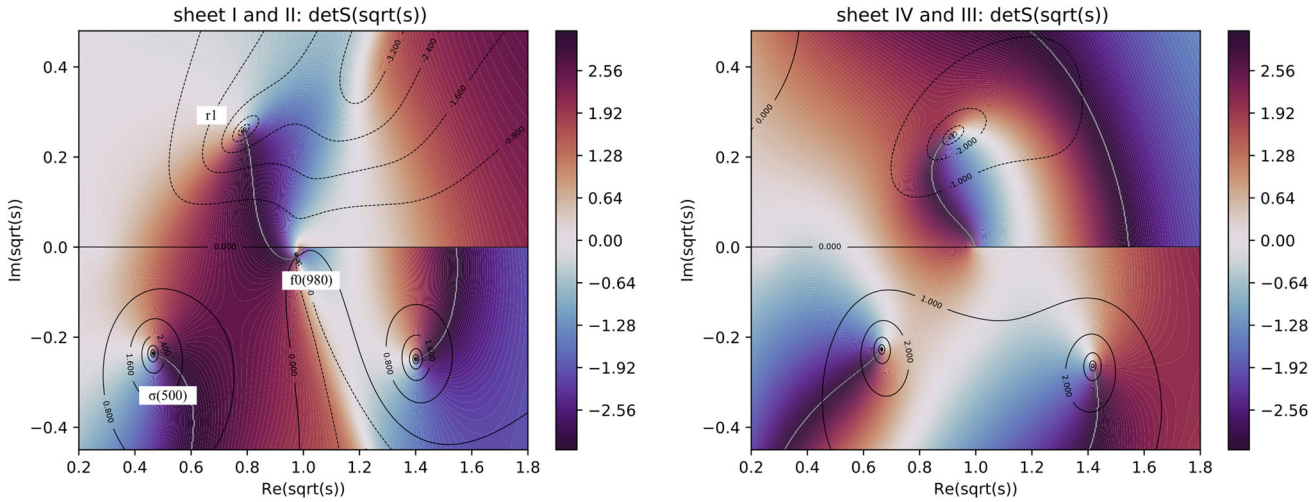

Fig. 1 Landscape of S-matrix phase $\ln\det S(\sqrt{s})$ of the $\pi\pi, K\bar{K}$ coupled-channel system on the energy sheets (left) I and II and (right) IV and III. See Table 1 for the definition of Riemann sheets. Color signifies the value of the phase angle and contour lines specify magnitudes of $\ln|\det S|$. Poles (roots) are characterized by the clockwise (anti-clockwise) rotation of the color phase and by a large, positive (negative) values of $\ln|\det S|$ reflected in the contour lines. The physical line is identified with the real line in sheet I ($\mathrm{Re}\,(\sqrt{s}) + i\,0^+$). The continuity of the phase across the Riemann sheets (see text): between sheet I and II (I and III) below (above) the $K\bar{K}$ threshold, is clearly visible as the continuity of color across the real line. Five resonances can be identified in this model: 3 on sheet II (left, bottom half) and 2 on sheet III (right, bottom half)

Table 1 Definition of Riemann sheets. Convention follows Ref. [16]

	$\mathrm{Im}\,q_{\pi\pi}$	$\mathrm{Im}\,q_{K\bar{K}}$
Sheet I	+	+
Sheet II	−	+
Sheet III	−	−
Sheet IV	+	−

$$V = \begin{bmatrix} g_{11} & g_{12} & g_{13} \\ g_{21} & g_{22} & g_{23} \\ g_{31} & g_{32} & 0 \end{bmatrix}. \tag{11}$$

The Lippmann–Schwinger equation can be easily solved by matrix inversion [4]:

$$\begin{aligned} G &= G^0 + G^0\,V\,G, \\ T &= V + V\,G^0\,T. \end{aligned} \tag{12}$$

The key step is the extraction of the S-matrix. It can be obtained by constructing the operator [3,4]:

$$\tilde{S} = (I - G^0_-\,V)\,(I + G^0_+\,T) \tag{13}$$

and projecting the upper 2×2 subspace of $\tilde{S}$. As we shall see, the contribution of the (dressed) resonance R and the existence of other dynamically generated states are contained within this projected S-matrix.

2.2 Phase of det S in the complex plane

Computing the S-matrix as a function of $\sqrt{s}$ in the complex plane, and evaluating the phase of det S, we obtain the plots in Fig. 1. This method of visualizing a complex function, called the domain coloring, is discussed in Ref. [17].

Although physical quantities are probed and extracted along the real line of $\sqrt{s}$, the plots display how the various S-matrix structures exert their influences. For example, an isolated pole (root) tends to rotate the phase in the clockwise (anti-clockwise) direction, but the actual influence on physical quantities depend on its distance to the real line and the Riemann sheet it is on. (See Table 1 for the definition of Riemann sheets.) In close proximity, a pole (or root) causes rapid phase motion, well described by a standard Breit–Wigner treatment. When probed afar, the influence becomes a non-trivial background which is generally non-negligible.

The phase shift function $\mathcal{Q}$ encapsulates the effects from various S-matrix objects on the real line. In Fig. 2 we show the result (black line) computed via the first line of Eq. (4). The same result can be obtained by directly reading off the value of the phase of detS from Fig. 1 along the physical line. (note the factor of 2)

We highlight some key features in these plots:

1. Five resonance poles are identified in this model, distributed across the Riemann sheets II (3 poles) and III (2 poles). It turns out that the density of states are only strongly influenced by three of the five poles: left 2 poles

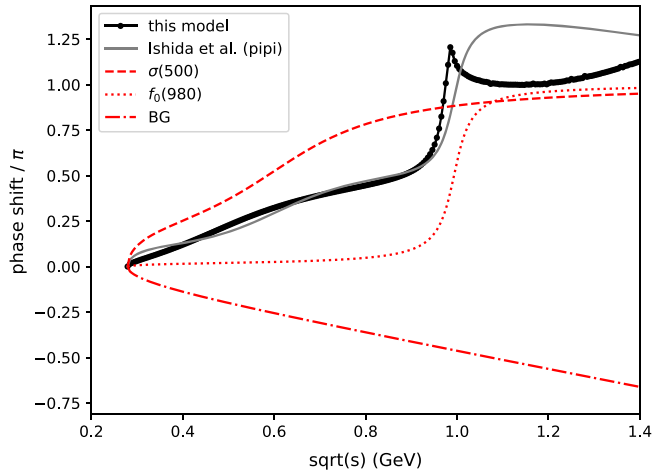

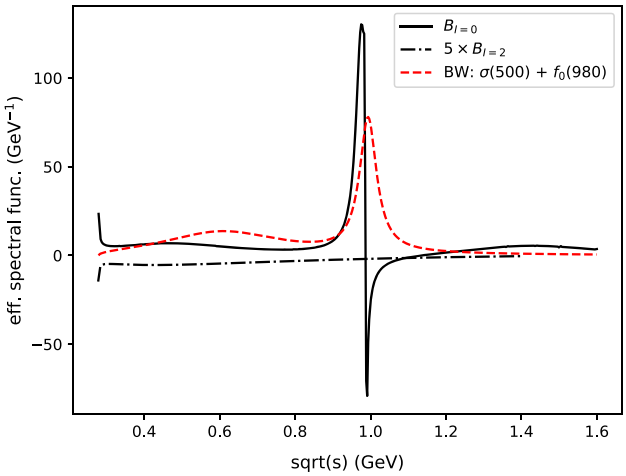

Fig. 2 Left: The effective phase shift extracted from the coupled-channel model, compared to the result of the model in Ref. [18]. For the latter, the decomposition of its components: $\sigma(500)$, $f_0(980)$ and a repulsive background, is also displayed. Right: The effective spectral function computed via Eq. (3). Also shown are the results of a (normalized) energy-dependent Breit–Wigner spectral functions based on the model in Ref. [18], and the $I = 2$ result computed using the experimental data in Ref. [19]

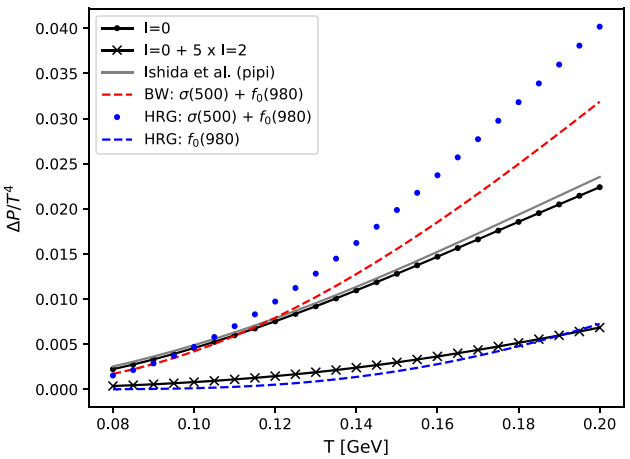

Fig. 3 Partial pressure (normalized to T^4) computed from various approximations of the density of states

on sheet II and the right pole on sheet III. This is naturally understood when considering the *continuity* of the phase of det S across the Riemann sheets.

2. The continuity can be understood as follows: In going across the real line from $i\,0^+$ to $-i\,0^+$, for Re $\sqrt{s}$ below the $K\bar{K}$ threshold, we essentially travel from sheet I to sheet II. Above the threshold, however, this becomes a transition from sheet I to sheet III. For the latter case, objects on sheet II would barely influence the real energy line. A similar conclusion is made for objects in sheet III in the former case. This gives an intuitive criteria for the relevance of poles (and roots) in the complex plane when calculating the physical density of states.
3. S-matrix roots are also important in determining the phase in the physical sheet. Their influence on channel amplitudes have been stressed in previous analyzes [20–22]. For the density of states, we find substantial contribution from various roots: e.g. $r_1 = (0.787 + i0.259)$ (GeV) sheet I.
4. Nature of resonances: Unlike the standard K-matrix approach, where resonance poles are introduced explicitly, the coupled-channel model considered here allows the dynamical generation of resonances. At physical couplings we expect the DoSs on the real line to be similar among different approaches (with suitably tuned model parameters). However the arrangement of poles and roots in the complex planes may be different. Also, it may be interesting to study the trajectory of the pole as couplings are altered: e.g. from zero to their physical values. In the current model, the five resonances are generated from a single bare state, and there is a distinct pattern in how, e.g. the $f_0(980)$ state (not a seed state) emerges.[1] Understanding such trajectory could be important for properly describing how shallow states are formed (and destroyed) in a thermal medium.

2.3 Thermal contribution of $\sigma(500)$ revisited

In the S-matrix formulation of statistical mechanics, the contribution to the thermal pressure by a state hinges on how rapid the phase motion it induces on the physical line. With the visualization method here (Fig. 1), this corresponds to

[1] The $f_0(980)$ resonance in this model starts off being a shallow bound state, generated within the $K\bar{K}$ channel. It then becomes a resonance due to the coupling to the $\pi\pi$ channel. This molecular origin gives a characteristic phase motion on $\mathcal{Q}$: a rapid rise similar to a standalone narrow state, accompanied by a rapid drop soon after.

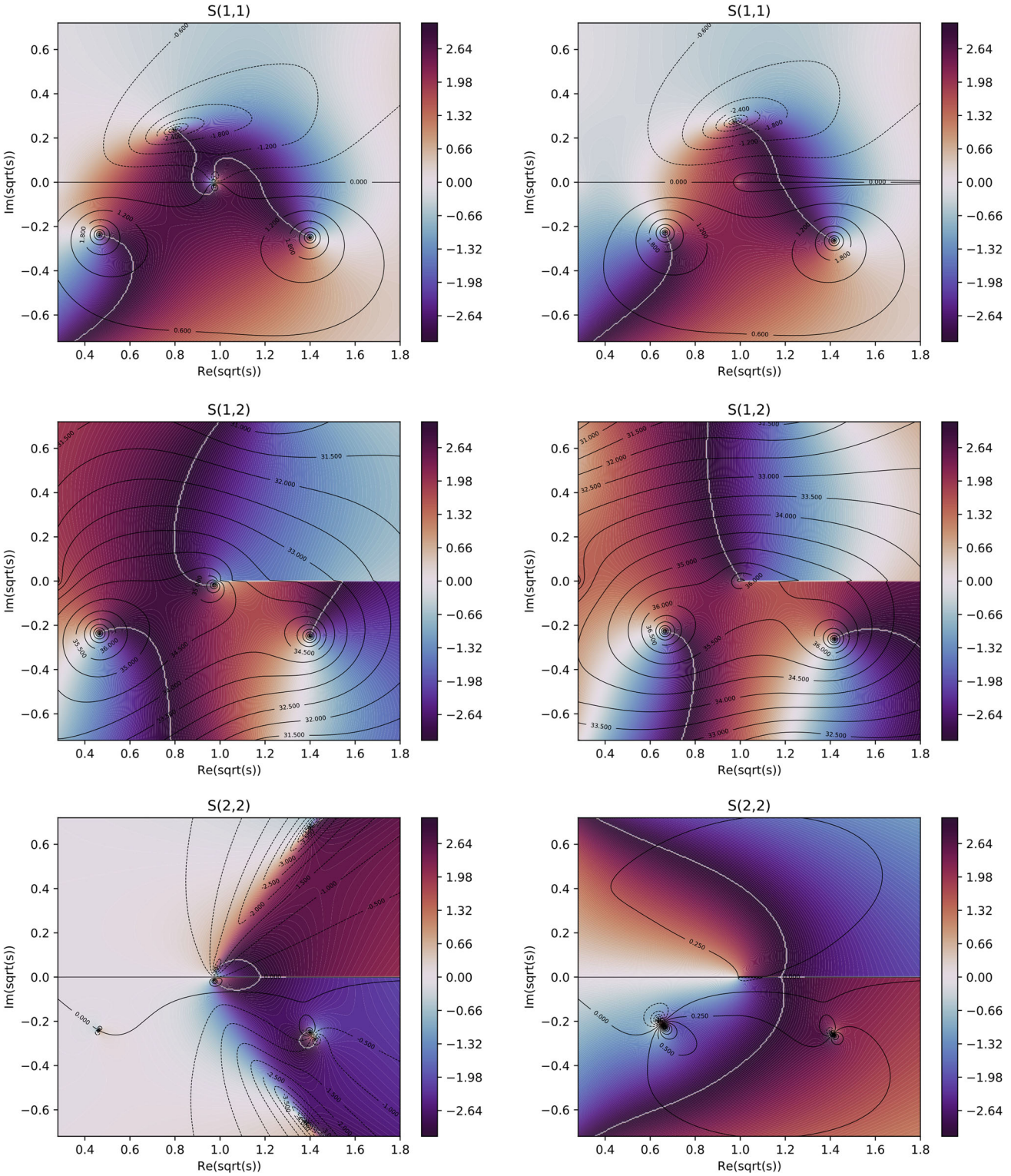

Fig. 4 Similar to Fig. 1 but for the S-matrix elements s_{11}, s_{12} and s_{22}. Observe the same pole structure appears, suggesting a common denominator function, but the numerators (containing roots) are different

how strongly the color is rotated by a given dynamical structure. For example, a broad resonance such as the $\sigma(500)$ state, tends to produce a smooth change as it is located further away from the real line.

While the net effect of all underlying structures can be identified with the measured phase shift, the decomposition into respective sources depends on the model. To gain further insights, we compare the result of the current coupled-channel model with another model of the $\pi\pi$ phase shift in Ref. [18]. This is summarized in Figs. 2 and 3.

1. Subtractive correction within the $I = 0$ channel: In the work of Ref. [18], a repulsive background is introduced, in addition to the resonant shifts of $\sigma(500)$ and $f_0(980)$, to reproduce the experimental phase shift. In the current model, this can be inferred from the mismatch of the r_1 root with the σ pole, giving a weaker phase motion. From Fig. 3, we see that the $I = 0$ partial pressure is significantly less than that of the sum of $\sigma(500)$ and $f_0(980)$, even after the widths are corrected for, i.e. as (energy-dependent) Breit–Wigner resonances using parameters of Ref. [18]. (The over-estimation is more severe when they are treated as point-like.) Thus we see the suppression of $\sigma(500)$ even within the $I = 0$ channel. Note that a repulsive component is also expected from t- and u-channel exchanges in chiral perturbation theory.
2. Model independence of thermal pressure: Despite the different decomposition into sources and backgrounds, both models roughly capture the experimental phase shift[2], and is sufficient to give a consistent result for the partial pressure. The small deviation seen between the two models is actually due to the repulsive $K\bar{K}$ component in the coupled-channel model, which is not accounted for in model [18]. This illustrates a powerful feature of the method: when the relevant experimental results are available to quantify the DoS, the results on thermal observables become model independent.
3. Adding the $I = 2$ interactions: The $I = 2$-channel of $\pi\pi$ scattering is known to be non-resonant and purely repulsive [19]. As we are dealing with the strong interaction, which preserves the isospin, the additional sector can be treated separately and the phase shift can be simply added (with a degeneracy factor five): the S-matrix is block-diagonal and the determinant factorizes. This subtractive contribution to the DoS (see Fig. 2 right) further reduces the thermal pressure to the level of the $f_0(980)$-only result (Fig. 3), and leads to the suggestion that $\sigma(500)$ should be excluded in the thermal model [14,23].

[2] The scattering length is not well captured by the model in Ref. [18]. It can be corrected using the techniques in Ref. [14].

3 Going further

Studying the phase of the det S reveals that particle dynamics is richer than pole hunting – roots and Riemann sheet structures can have important (sometimes dominant) effects on the density of states.

In a transparent model like this, where the complete information of the S-matrix is available, the contribution from each object to the effective phase shift on the real line can be tracked. Of course, there exist more sophisticated models for describing the $\pi\pi$, $K\bar{K}$ system, which respect the chiral symmetry principles [24–26]. The aim here is not so much about explaining the scattering data, but to make use of this familiar example to study how dynamical structures exert their influences on the DoS, and building on these insights to invent a more robust approximation scheme for thermal models. For example, based on the analysis of the Riemann sheets and the continuity of the effective phase shift function, we can select the most relevant poles and roots in the complex plane, and construct an HRG-like approximation scheme for calculating the density of states [15].

Given the large number of predicted states (e.g. by LQCD [27]) which are unobserved, and the observed states which are unconfirmed in experiments, a criterion for selecting the most relevant states in constructing the density of states is urgently needed [28,29], This is also essential for reliably describing the thermodynamics at high temperatures and densities [30]. We can imagine a scenario where some of the bound states predicted from a quark model calculation, after coupling to the continuum (i.e., open channels), they are so redistributed that they have little influence on the density of states. This issue should be dealt with, regardless of the width of the resonance.

It would also be useful to explore other interacting system. Thermodynamics of system of exotics [31] would be a good testing ground, where a coupled-channel study is mandatory. A good example of this is the X(3872) system. Previous works have focused on the single channel phase shift [32,33]. Our study here suggests that analyzing the structure of det S may yield a better understanding for characterizing the density of states.

Acknowledgements The author thanks Eric Swanson for stimulating discussions. He also acknowledges fruitful discussions with Hans Feldmeier and Bengt Friman. This study receives supports from the Short Term Scientific Mission (STSM) program under COST Action CA15213 (reference number: 41977) and the Polish National Science Center (NCN) under the Opus grant no. 2018/31/B/ST2/01663.

Data Availability Statement This manuscript has no associated data or the data will not be deposited. [Authors' comment: Data sharing is not applicable to this article as no new data were created.]

Complex landscapes of S-matrix elements

In the present model we can also study the complex planes of an individual S-matrix element: s_{11}, s_{12} and s_{22}. It is useful to understand the entry as a quotient of two functions: $N(z)/D(z)$: the denominator D contains the pole information, and is expected to be common among all matrix elements (seen to be the case from direct computation), but the numerator functions N's are expected to be different. Note that the DoS of the system is extracted from the combination $s_{11}s_{22} - s_{12}s_{21}$, i.e., the determinant.

References

1. R. Dashen, S.-K. Ma, H.J. Bernstein, S Matrix formulation of statistical mechanics. Phys. Rev. **187**, 345–370 (1969)
2. R. Venugopalan, M. Prakash, Thermal properties of interacting hadrons. Nuclear Phys. A **546**(4), 718–760 (1992)
3. P.M. Lo, S-matrix formulation of thermodynamics with N-body scatterings. Eur. Phys. J. C **77**(8), 533 (2017)
4. P.M. Lo, F. Giacosa, Thermal contribution of unstable states. Eur. Phys. J. C **79**(4), 336 (2019)
5. P. Gerber, H. Leutwyler, Hadrons below the chiral phase transition. Nuclear Phys. B **321**(2), 387–429 (1989)
6. J.A. Oller, E. Oset, J.R. Pelaez, Meson-meson interaction in a non-perturbative chiral approach. Phys. Rev. D **59**, 074001 (1999). Erratum-ibid.D60:099906,1999; Erratum-ibid.D, 75:099903, 2007
7. W. Weinhold, B. Friman, W. Norenberg, Thermodynamics of Delta resonances. Phys. Lett. **B433**, 236–242 (1998)
8. R. Hagedorn, Statistical thermodynamics of strong interactions at high-energies. Nuovo Cim. Suppl. **3**, 147–186 (1965)
9. A. Andronic, P. Braun-Munzinger, K. Redlich, J. Stachel, Decoding the phase structure of QCD via particle production at high energy. Nature **561**(7723), 321–330 (2018)
10. P.M. Lo, Resonance decay dynamics and their effects on p_T-spectra of pions in heavy-ion collisions. Phys. Rev. C **97**(3), 035210 (2018)
11. V.E. Markushin, The Radiative decay phi → gamma pi pi in a coupled channel model and the structure of f(0)(980). Eur. Phys. J. A **8**, 389–399 (2000)
12. M.P. Locher, V.E. Markushin, H.Q. Zheng, Structure of f0 (980) from a coupled channel analysis of S wave pi pi scattering. Eur. Phys. J. C **4**, 317–326 (1998)
13. D. Morgan, M.R. Pennington, New data on the K anti-K threshold region and the nature of the f0 (S*). Phys. Rev. D **48**, 1185–1204 (1993)
14. B. Friman, P.M. Lo, M. Marczenko, K. Redlich, C. Sasaki, Strangeness fluctuations from $K - \pi$ interactions. Phys. Rev. D **92**(7), 074003 (2015)
15. P.M. Lo, Density of states of a coupled-channel system. Phys. Rev. D **102**, 034038 (2020)
16. A.M. Badalyan, L.P. Kok, M.I. Polikarpov, Y.A. Simonov, Resonances in coupled channels in nuclear and particle physics. Phys. Rep. **82**(2), 31–177 (1982)
17. E. Wegert, *Visual Complex Functions: An Introduction with Phase Portraits* (Bücher. Springer Basel, SpringerLink, 2012)
18. S. Ishida, T. Ishida, M. Ishida, K. Takamatsu, T. Tsuru, Further analysis on bcy particle properties. Prog. Theor. Phys. **98**(4), 1005–1010 (1997)
19. C.D. Froggatt, J.L. Petersen, Phase-shift analysis of $\pi + \pi -$ scattering between 1.0 and 1.8 gev based on fixed momentum transfer analyticity (ii). Nuclear Phys. B **129**(1), 89–110 (1977)
20. R. Kaminski, L. Lesniak, B. Loiseau, Scalar mesons and multichannel amplitudes. Eur. Phys. J. C **9**, 141–158 (1999)
21. R. Kaminski, L. Lesniak, J.P. Maillet, Relativistic effects in the scalar meson dynamics. Phys. Rev. D **50**, 3145–3157 (1994)
22. D. Ronchen, M. Doring, F. Huang, H. Haberzettl, J. Haidenbauer, C. Hanhart, S. Krewald, U.G. Meissner, K. Nakayama, Coupled-channel dynamics in the reactions piN → piN, etaN, KLambda. KSigma. Eur. Phys. J. **A49**, 44 (2013)
23. W. Broniowski, F. Giacosa, V. Begun, Cancellation of the σ meson in thermal models. Phys. Rev. C **92**(3), 034905 (2015)
24. J.R. Peláez, The su(2) and su(3) chiral phase transitions within chiral perturbation theory. Phys. Rev. D **66**, 096007 (2002)
25. A. Gómez Nicola, J.R. Peláez, Meson-meson scattering within one-loop chiral perturbation theory and its unitarization. Phys. Rev. D **65**, 054009 (2002)
26. J.R. Pelaez, Light scalars as tetraquarks or two-meson states from large N(c) and unitarized chiral perturbation theory. Mod. Phys. Lett. A **19**, 2879–2894 (2004)
27. R.A. Briceno, J.J. Dudek, R.D. Young, Scattering processes and resonances from lattice QCD. Rev. Mod. Phys. **90**(2), 025001 (2018)
28. P.M. Lo, M. Marczenko, K. Redlich, C. Sasaki, Matching the Hagedorn mass spectrum with Lattice QCD results. Phys. Rev. C **92**(5), 055206 (2015)
29. J. Cleymans, P.M. Lo, K. Redlich, N. Sharma, Multiplicity dependence of (multi-)strange baryons in the canonical ensemble with phase shift corrections. Phys. Rev. C **103**(1), 014904 (2021)
30. C. Fernndez-Ramrez, P.M. Lo, P. Petreczky, Thermodynamics of the strange baryon system from a coupled-channels analysis and missing states. Phys. Rev. C **98**(4), 044910 (2018)
31. R.F. Lebed, R.E. Mitchell, E.S. Swanson, Heavy-Quark QCD Exotica. Prog. Part. Nucl. Phys. **93**, 143–194 (2017)
32. P.G. Ortega, D.R. Entem, F. Fernandez, E.R. Arriola, Counting states and the Hadron resonance gas: does X(3872) count? Phys. Lett. B **781**, 678–683 (2018)
33. F. Giacosa, M. Piotrowska, S. Coito, $X(3872)$ as virtual companion pole of the charm-anticharm state $\chi_{c1}(2P)$. Int. J. Mod. Phys. A **34**(29), 1950173 (2019)